Eur. Phys. J. B **61**, 25–31 (2008)
DOI: 10.1140/epjb/e2008-00025-1

THE EUROPEAN PHYSICAL JOURNAL B

Effect of oxygen deficiency on the radiation sensitivity of sol-gel Ge-doped amorphous SiO_2

S. Agnello[1,a], A. Alessi[1], F.M. Gelardi[1], R. Boscaino[1], A. Parlato[2], S. Grandi[3], and A. Magistris[3]

[1] Department of Physical and Astronomical Sciences, University of Palermo, via Archirafi 36, 90123, Palermo, Italy
[2] Department of Nuclear Engineering, University of Palermo, Viale delle Scienze, Building 6, 90128 Palermo, Italy
[3] Department of Physical Chemistry, University of Pavia, via Taramelli 16, 27100, Pavia, Italy

Received 7 September 2007 / Received in final form 19 November 2007
Published online 18 January 2008 –

Abstract. We report experimental investigation by electron paramagnetic resonance (EPR) measurements of room temperature γ-ray irradiation effects in sol-gel Ge doped amorphous SiO_2. We used materials with Ge content from 10 up to 10^4 part per million (ppm) mol obtained with different preparations. These latter gave rise to samples characterized by different extents of oxygen deficiency, estimated from the absorption band at ∼5.15 eV of the Ge oxygen deficient centers (GeODC(II)). The irradiation at doses up to ∼400 kGy induces the E'-Ge, Ge(1) and Ge(2) paramagnetic centers around $g \sim 2$ with concentrations depending on Ge and on GeODC(II) content. We found correlation between Ge(2) and GeODC(II) contents, supporting the suggestion that the latter defect is the precursor of Ge(2). Even if the concentration of E'-Ge and Ge(1) defects cannot be strictly related to GeODC(II) one, the concentration growth of these paramagnetic defects with irradiation evidences that the radiation sensitivity is enhanced by the oxygen deficiency for Ge doping above 1000 ppm mol and it is reduced below 100 ppm mol. Moreover, the investigation of samples with different GeODC(II) concentration but fixed Ge content has shown that the oxygen deficiency enhances the overall radiation sensitivity for [GeODC(II)]/[Ge] in the range $10^{-3} \div 10^{-2}$.

PACS. 61.72.Hh Indirect evidence of dislocations and other defects (resistivity, slip, creep, strains, internal friction, EPR, NMR, etc.) – 61.80.Ed Gamma-ray effects – 71.55.Jv Disordered structures; amorphous and glassy solids

1 Introduction

Several studies about point defects in Ge-doped amorphous SiO_2 materials regard the optical absorption (OA) band located at ∼5.15 eV (called $B_{2\beta}$ band) [1–4], characterized by a full width at half maximum (*FWHM*) of ∼0.5 eV, and two related photoluminescence (PL) bands observed at ∼3.2 eV and ∼4.3 eV [2,4]. This overall optical activity has been related to the oxygen deficiency of the material and the associated point defect has been generally named Ge oxygen deficient center, or GeODC(II) [3,4]. The twofold coordinated Ge:O – $\overset{\bullet\bullet}{\text{Ge}}$ – O (where – represents a bond between Ge and O, and •• is an electron lone pair), was proposed by Skuja as the responsible center of these OA and PL activities [4]. In another model the oxygen divacancy was proposed by Tsai et al. as the center responsible for the $B_{2\beta}$ and the related PL bands [5]. In a further structural model it is suggested that an oxygen vacancy involving a Ge atom [6,7], or an intrinsic oxygen deficient center with optical properties modified by a near Ge atom, can be the origin of the $B_{2\beta}$ band [8]. Up until recently, literature contains references to the twofold coordinated center and to the oxygen vacancy models and no definitive structure has been universally accepted for the GeODC(II).

The presence of oxygen deficient centers (ODC) has been suggested to play a relevant role in the interaction of Ge-doped silica with ionizing radiation since it increases the material photo-sensitivity [1,3,9,10]. In the interaction of radiation with Ge-doped silica new defects are induced. Within the context of photo-sensitivity and second-order optical non-linearity, among the most relevant of the induced defects are those usually named Ge(1), Ge(2) and E'-Ge. Indeed, they are responsible for optical absorption changes in the spectral range between 4 eV and 6.5 eV, and consequently they induce modification of the refractive index [1,3,10]. All of the above defects are also paramagnetic giving rise to electron paramagnetic resonance (EPR) signals at $g \sim 2$ [1,3]. The Ge(1) center is supposed to be formed by an electron trapped in a tetra-coordinated Ge atom [11,12]. The structural model of E'-Ge center consists of a threefold-coordinated Ge atom with an unpaired electron: $O \equiv Ge^{\bullet}$ (where ≡ represents single bonds with three oxygen atoms, and • is an unpaired

[a] e-mail: agnello@fisica.unipa.it

Table 1. Sample nicknames; nominal Ge content in part per million molar and in atoms for cm^3; content of Ge estimated from instrumental neutron activation analysis (INAA) [17]; content of GeODC(II) estimated from OA and PL spectra (N.D. means concentration below the PL detection limit $\sim 4 \times 10^{15}$ centres/cm^3); GeODC(II) concentration ratio with respect to Ge content.

Sample	Ge (ppm mol)	Ge atoms (cm^{-3})	Ge (ppm mol) INAA reference [17]	GeODC(II) (centers/cm^3)	[GeODC(II)]/[Ge]
A1	10 000	2.2×10^{20}		$(1.5 \pm 0.5) \times 10^{17}$	$\sim 10^{-3}$
A2	10 000	2.2×10^{20}		N.D.	$< 10^{-4}$
A3	10 000	2.2×10^{20}		$(5 \pm 2) \times 10^{18}$	$\sim 10^{-2}$
B3	1000	2.2×10^{19}	818 (±0.7%)	$(4.5 \pm 1.4) \times 10^{17}$	$\sim 10^{-2}$
C3	100	2.2×10^{18}	77 (±1.5%)	$(7 \pm 2) \times 10^{16}$	$\sim 10^{-2}$
D3	10	2.2×10^{17}	12 (±8.5%)	N.D.	–

electron) [5,11,13]. Even if more contrasted, it has been proposed that the most probable structural model for the Ge(2) center consists in a ionized twofold coordinated Ge obtained by releasing one electron: $O - \dot{G}e - O$ [14].

Even though many years of research have produced a lot of data about the generation of the above centers, today a real understanding of conversion and creation mechanisms has not been obtained yet. In fact, it has been proposed that ODC are involved but there is not a clear picture about the way they take part in optical modifications and in photo-processes involving Ge related paramagnetic point defects. For example, some data suggest that the GeODC(II) can be precursor of Ge(2) involving also the Ge(1) [14], but the Ge(1) creation in low ODC content samples is an evidence that a channel independent from oxygen deficiency exists [15].

In the present work we experimentally investigate the effects of gamma ray irradiation on various sol-gel materials with Ge doping varying from 10 up to 10^4 part per million (ppm) molar covering a range poorly studied up to now. Since the usually employed materials have some percent molar of Ge [1,10] and the samples here investigated are characterized by different oxygen deficiency as estimated by the concentration ratio [GeODC(II)]/[Ge], by their investigation we can elucidate the effective role of the lack of oxygen with respect to the role of the Ge atoms concentration on the photo-sensitivity of the material.

2 Experimental

The employed materials are sol-gel Ge doped SiO_2 that are obtained from weighted mixtures of TEOS (tetra-etil-orthosilicate) and TEOG (tetra-etil-orthogermanate). The densification of the obtained aerogels was carried out employing different temperature routes and atmospheres. In details, sample A1 reported in Table 1, was obtained by heating at a rate 0.3 °C/min up to 1200 °C, then was kept at 1200 °C for 0.75 h and finally was cooled down to room temperature. During heating O_2 and N_2 flux was kept up to 800 °C then He flux, and finally N_2 flux during cooling. Sample A2 had the same route as A1 but the atmosphere was changed to air from 800 °C onward. The samples named A3, B3, C3 and D3 were heated with a rate of 0.3 °C/min from 25 °C to 1150 °C, then they were kept at this temperature for 24 hours before returning to room temperature. An O_2 flux was used until 700 °C, while a low pressure atmosphere ($\sim 10^{-5}$ atm) was used during the other part of the densification process.

From the synthesis we obtained cylindrical shape specimens that were cut to obtain samples in disks of typical diameter ∼4.7 mm and thickness ∼0.7 mm with the largest surfaces optically polished.

The γ irradiation was done at room temperature in a ^{60}Co source. The growth of paramagnetic defects concentration as a function of exposure time was studied for doses ranging from 5 Gy up to 420 kGy in each material employing a dose rate ∼64 Gy/h up to 50 Gy and then a dose rate ∼1.7 kGy/h. The doses were accumulated progressively in one sample for each of the studied materials.

The EPR measurements were recorded at room temperature using a Bruker EMX spectrometer working at 9.8 GHz. All the measurements were done using a modulation magnetic field with frequency of 100 kHz while all the other experimental parameters were regulated so that the EPR signal was not distorted nor saturated by the microwave power. To estimate the paramagnetic centers concentration the double integral of their EPR signal was determined and was compared to that of a reference sample having the same dimensions and containing a known concentration of E'-Si centers [16].

The optical measurements were carried out at room temperature. OA measurements have been made in the spectral range 2–6 eV using a spectrophotometer Jasco V-560. For the PL measurements a spectrofluorometer Jasco FP6500 has been employed using a 150 W Xenon lamp source. The scan time was fixed in order to avoid both distortion of the detected bands and excessive exposure of the sample to the UV source since it could induce photo-processes. For the PL measurements the samples were placed in a 45° back scattering configuration and the acquired spectra were corrected for the spectral efficiency of the detection system and for the spectral dispersion.

2.1 Pre-irradiation measurements

In Figure 1 a typical OA spectrum is reported as recorded in the as-prepared A1 sample. A band peaked at (5.13 ± 0.02) eV with FWHM (0.46 ± 0.02) eV is clearly distinguishable. The PL spectrum of the same sample excited at

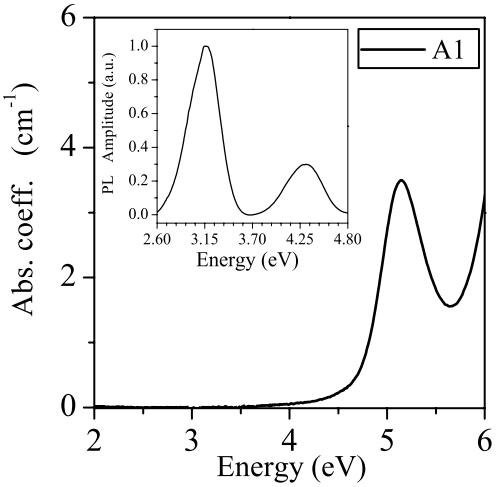

Fig. 1. Absorption spectrum recorded in the as-prepared A1 sample in the range 2–6 eV; in the inset we report the PL spectrum recorded in the same sample under excitation energy at 5.0 eV.

5.0 eV showing two emission bands peaked at 4.3 eV and at 3.2 eV, is reported in the inset of the figure. This overall optical activity is in good agreement with the characteristic bands tied to the GeODC(II). Similar optical measurements carried out in the other samples have allowed us to detect and estimate the concentration of GeODC(II). The obtained results are summarized in Table 1 where it is shown that GeODC(II) are detected in samples A1, A3, B3 and C3, while in samples A2 and D3 they, if present, are in a concentration that is below the instrumental sensibility. It is worth to note that the oscillator strength value used for these concentration estimations is 0.1 as reported in [18–20] for the $B_{2\beta}$ optical absorption band. Furthermore, when this OA band was below the detection limit but the associated PL bands were observed, the GeODC(II) content was estimated from these latter as the PL measurements become quantitative for absorption coefficient below 1 cm^{-1} [1]. The ratio between GeODC(II) defects concentration and the nominal content of Ge is of the order of 10^{-2} in the A3, B3, C3, D3 samples, while for the samples A1 and A2, having a different densification history, such ratio is of the order of 10^{-3} or lower. Since the GeODC(II) content can be considered a marker of the oxygen deficiency of the material, from the above ratio a different oxygen deficiency of the samples with 10^4 ppm mol Ge is deduced. No EPR signal was observed in as-prepared samples.

3 Experimental results

The samples have been investigated carrying out EPR measurements in the region $g \sim 2$ after each irradiation session. In Figure 2a, we report a typical EPR spectrum as recorded in the sample A3 irradiated at the dose of 160 Gy. The spectrum shows a composite structure from 346 mT up to 348 mT, that suggests the presence of both

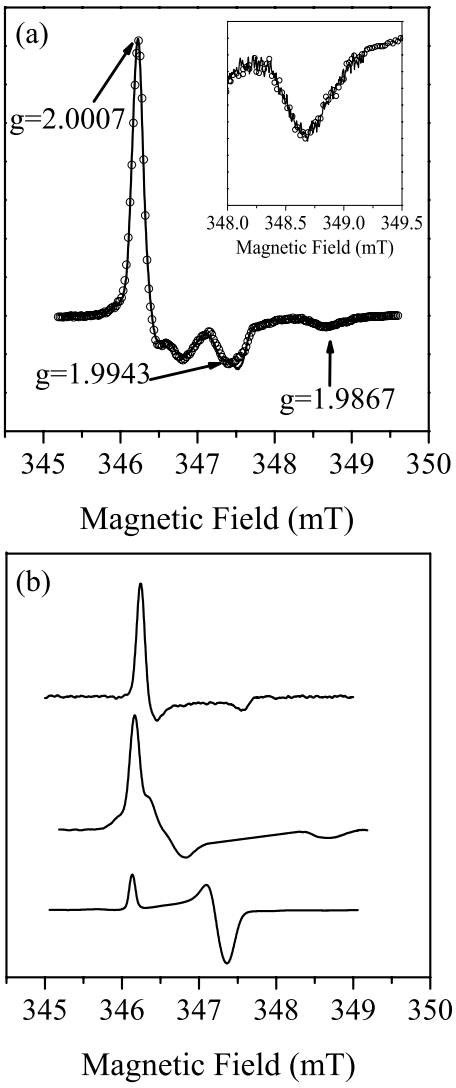

Fig. 2. (a) EPR spectrum recorded in sample A3 at 160 Gy, full line, and line shape obtained by summing Ge(1), Ge(2) and E'-Ge signals, open circles; (b) from top to bottom, line shapes of Ge(1), Ge(2) and E'-Ge used for experimental spectrum decomposition.

E'-Ge and Ge(1) centers [13,21], and an isolated feature at 348.7 mT attributable to the presence of Ge(2) [13].

In order to elucidate the presence of the different Ge related centers, a decomposition of the acquired spectrum has been done using the reference line shapes for E'-Ge, Ge(1) and Ge(2) centers shown in Figure 2b. The line shape for E'-Ge was obtained in a 2% Ge-doped silica sol-gel sample UV irradiated. In this material we have observed a isolated signal having the same line shape reported in literature for E'-Ge [22]. The Ge(1) reference line shape was isolated in a sample of the material A1 irradiated at 1 kGy. After irradiation this material has been isochronally thermally treated in the temperature range between 25 °C and 140 °C where the features of the other paramagnetic centers did not change in agreement with literature data [3]. From the difference of the spectra

Table 2. Value of g estimated for Ge(1), Ge(2) and E'-Ge using g_2 value of E'$_\gamma$ -Si as reference [23]; the error on all g values estimation is 0.0003.

	g_1	g_2	g_3
Ge(1)	2.0006	2.0000	1.9930
Ge(2)	2.0010	1.9989	1.9867
E'-Ge	2.0012	1.9951	1.9941

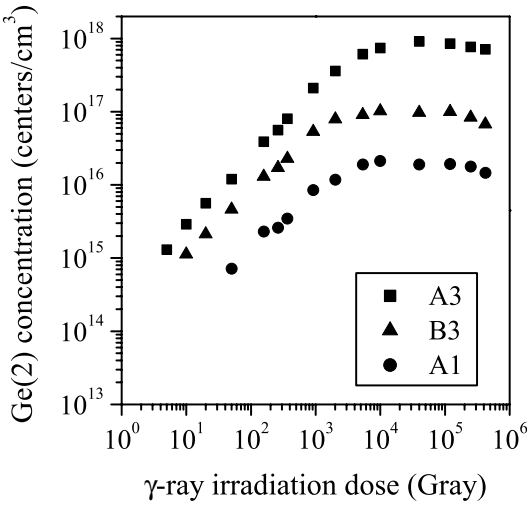

Fig. 3. Concentration of Ge(2) paramagnetic centers in samples A1 (•), A3 (■), B3 (▲) as a function of the dose.

during this thermal treatment it was possible to isolate the Ge(1) signal. It is worth to note that in this sample no Ge(2) signal was detected making easier to isolate the Ge(1) one. Finally, the Ge(2) center reference line shape was determined from the residual of the decomposition of the spectrum in Figure 2a with the above described reference line shapes of Ge(1) and E'-Ge centers. As shown in Figure 2a, the result of this decomposition procedure is in good agreement with the experimental signal and of comparable quality with those usually reported in literature [13].

The g-values of the obtained reference line shapes are reported in Table 2 and are in good agreement with those reported in literature [13,14,22] apart from the g_2 value of Ge(1) and Ge(2) centers. It is worth to note that this mismatch could be due to the fact that in [13] the latter line shapes have been determined by fitting an experimental spectrum with simulated EPR lines of the two centers.

The above decomposition has been applied to all the acquired spectra and the presence of these three kinds of paramagnetic defects has been investigated as a function of the accumulated dose in the various samples with an error in the estimated signals amplitude of 10%.

The Ge(2) paramagnetic centers have been detected in samples A1, A3 and B3, their presence being clearly identified by the spectral feature at 348.7 mT. The growth of Ge(2) concentration, as determined by the above described decomposition, is reported in Figure 3. All the samples show a dose range in which the concentration increases linearly with dose, then a limit value is reached followed by a slight concentration decrease. The limit value attained depends on the sample and increases with the GeODC(II) initial content.

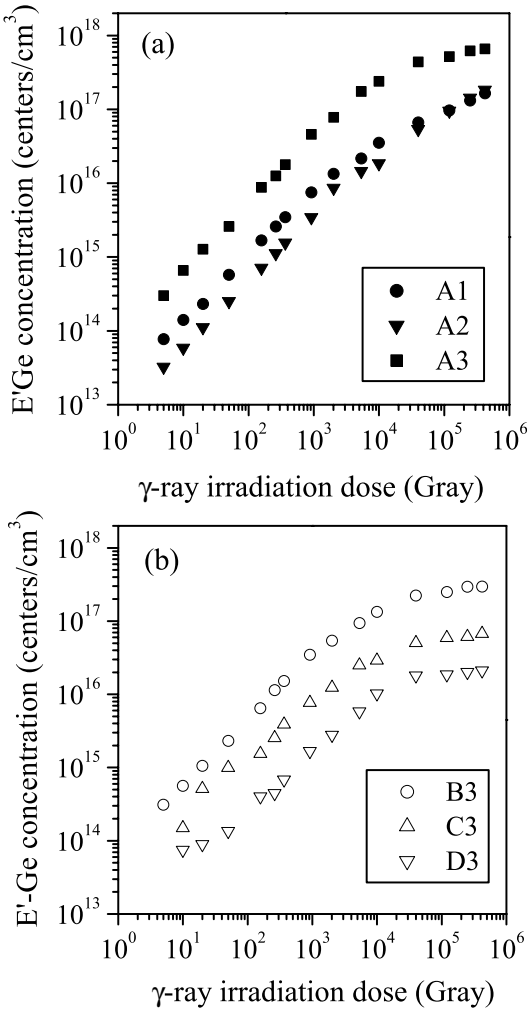

Fig. 4. Concentration of E'-Ge defects as a function of dose in samples (a) A1(•), A2(▼), A3(■); (b) B3(◯), C3(△), D3(▽).

As shown in Figure 4, the E'-Ge centers were detected in all of our samples, with a concentration depending on the kind of material and on the dose. In the materials with 10^4 ppm mol of Ge (Fig. 4a), the E'-Ge centers concentration increases linearly with dose up to $\sim 10^3$ Gy with an efficiency increasing with the GeODC(II) content. For higher doses the growth rate decreases but no limit value was observed in the three materials. In Figure 4b, we report the concentration growth of E'-Ge defects in samples doped with different amounts of Ge atoms. Also in this case the E'-Ge centers increase linearly with dose up to $\sim 10^3$ Gy in all the materials and their concentration depends on Ge content. For higher doses, and Ge content $\leqslant 10^3$ ppm, these defects attain a limit value.

The growth of Ge(1) centers concentration is reported in Figure 5a for the samples doped with 10^4 ppm mol of Ge, and in Figure 5b for the other samples. Also this kind of defects has concentration that increases in all the

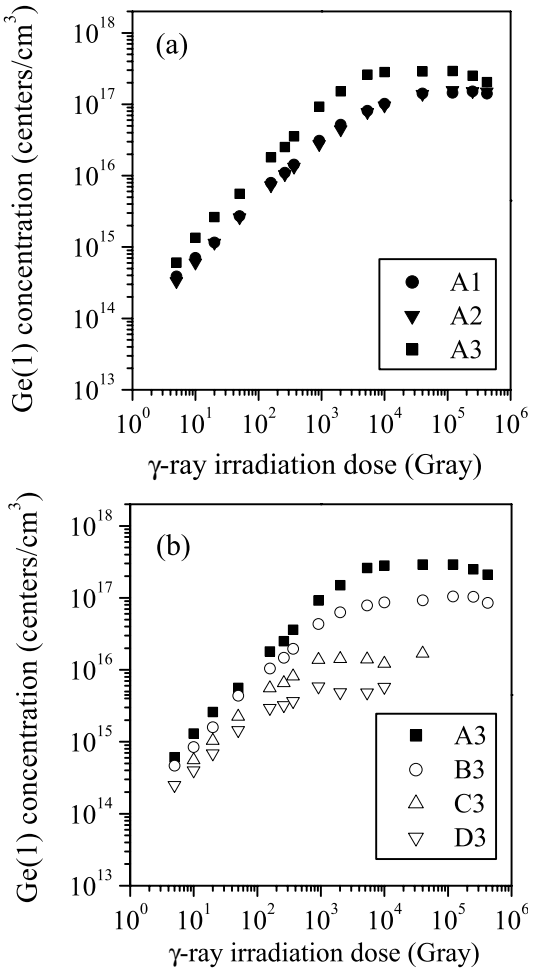

Fig. 5. Concentration of Ge(1) centers as a function of dose in samples (a) A1(●), A2(▼), A3(■); (b) A3(■), B3(◯), C3(△), D3(▽).

samples at low doses, tends to a limit value on increasing the dose and then show a slight decrease. There is not difference in the induced Ge(1) centers in samples A2 and A1, while in sample A3 they are found in higher concentration for all the investigated doses. As evidenced in Figure 5b, for the materials with $\frac{[\text{GeODC(II)}]}{[\text{Ge}]} \sim 10^{-2}$ the Ge(1) content changes with the different Ge contents. The missing points at high doses in samples C3 and D3 are due to the low concentration of Ge(1) and the overlap with the resonance signal of the E'-Si center [23], induced in this range of doses, that prevents a correct estimation of the Ge(1) signal intensity.

4 Discussion

In the samples A1, A3, B3 with concentration of GeODC(II) above 10^{17} centers/cm^3 the Ge(2) centers have been observed after irradiation and they reach a limit value for doses above $\sim 10^4$ Gy. The limit concentration of these latter defects is approximately 15% of the initial concentration of GeODC(II). Even if we cannot justify with our current understanding this ratio, comparing the reported results for the sample A1 (see Fig. 3) with those for A3 and B3, it can be observed that the Ge(2) centers generation is linked only to the presence of GeODC(II) and is not affected by the Ge content. Indeed, the first two samples have the same concentration of Ge but differ in that of GeODC(II) and the efficiency of Ge(2) generation is correlated to this latter. Similarly, the B3 sample has lower Ge content than A1 but its GeODC(II) content is higher and also that of induced Ge(2). These experimental observations enforce the model that assumes the GeODC(II) as precursor of Ge(2) defect, the conversion occurring by an ionization process as already proposed [14]: GeODC(II) $\xrightarrow{h\nu}$ Ge(2) + e$^-$, where e$^-$ represents a released electron.

As shown in Figure 4a, the presence of oxygen deficiency, as derived from the GeODC(II) content, affects the generation of E'-Ge centers at fixed Ge content of 10^4 ppm, suggesting that a generation process of E'-Ge involving oxygen deficient precursors is effective. This is not surprising if, as expected, the E'-Ge are generated from native oxygen monovacancies, through, for example, the radiation ionization of vacancies involving a Ge atom:

$$\text{O} \equiv \text{Ge–T} \equiv \text{O} \xrightarrow{h\nu} \text{O} \equiv \text{Ge}^{\bullet}\text{T} \equiv \text{O} + \text{e}^-,$$

where T represents a Si or Ge atom. This relevant role of the oxygen deficiency can be further pointed out by observing that the sample B3 has more E'-Ge centers than samples A1 and A2 that have higher Ge content but lower oxygen deficiency.

We note that the samples A1 and A2 have slightly different concentration growth below 10^4 Gy and a similar one at larger doses. This feature shows that other mechanisms not depending on native oxygen deficiency could be also effective and are evidenced when the conversion processes involving oxygen deficient precursors are exhausted. This effect is less relevant in the growth curve of the sample A3, probably because of the higher concentration of native oxygen deficient precursors.

From the growth curves of Ge(1) and Ge(2) centers in samples A1, A3 and B3 we can calculate the ratio between the concentration of these two kinds of defects. We note that this ratio is ∼6 in sample A1, ∼0.5 in sample A3 and ∼1 in sample B3. These data show that there is not univocal correlation between Ge(2) and Ge(1) so that we can exclude that the process of ionization of GeODC(II) and a consequent trapping of the electron in a substitutional Ge, already suggested [14]: GeODC(II) + O=Ge=O $\xrightarrow{h\nu}$ Ge(2) + Ge(1), (where = represents single bonds to two different O atoms) is the only effective in generating Ge(2) and Ge(1). In particular, in the A3 sample there are electrons released from GeODC(II) that are not trapped in substitutional fourfold coordinated Ge atoms in agreement with other experimental observations [9].

The comparison of samples A1, A2, A3 in Figure 5a evidences that the induced Ge(1) centers depend on the oxygen deficiency ratio to Ge content. In details, differences of efficiency of Ge(1) centers generation occurs when $\frac{[\text{GeODC(II)}]}{[\text{Ge}]} > 10^{-3}$, and it can be observed that more Ge(1)

are induced on increasing the oxygen deficiency. This result can be explained in a frame in which the GeODC(II) sites, under irradiation, release electrons (we call them a-type electrons) that can be trapped by fourfold coordinated Ge sites forming Ge(1) centers, in addition to that ones coming from other donor sites (b-type electrons) in the glassy matrix. On these bases it is not surprising that in A3 sample more Ge(1) defects are generated with respect to the other two samples, due to a larger contribution of a-type electrons coming from GeODC(II) sites. At variance, the superposition of the Ge(1) growth curves in A1 and A2 samples can be due to a too low contribution of a-type electrons, so that the final Ge(1) concentration is fixed by the exhaustion of b-type electrons, independently from the GeODC(II) concentration. Quantitatively, in sample A3 there are $\sim 10^{18}$ GeODC(II) donors and the final Ge(1) concentration is $\sim 3 \times 10^{17} \mathrm{cm}^{-3}$, whereas in A1 and A2 in front of a slightly lower Ge(1) concentration ($\sim 10^{17} \mathrm{cm}^{-3}$) the GeODC(II) concentrations are lower by at least by one and two orders of magnitude, respectively.

By observing Figure 5b, we note a different dependence on dose of the induced Ge(1) defects for various Ge contents, even if the oxygen deficiency ratio $\frac{[\mathrm{GeODC(II)}]}{[\mathrm{Ge}]}$ is fixed to $\sim 10^{-2}$ in all the samples. In particular the saturation value appears more dependent on Ge, and as consequence on GeODC(II), then the growth rate. The latter finding is in disagreement with previous results reported in [15], where no differences were found in samples with $\frac{[\mathrm{GeODC(II)}]}{[\mathrm{Ge}]} \sim 10^{-4}$. In fact, the samples studied in [15] showed the same growth curves of Ge(1) independently on the Ge content from 10 up to 10^4 ppm mol. From this comparison we could argue that in samples reported in the present study the spread in Ge(1) concentration for the different Ge amounts, is due to a larger $\frac{[\mathrm{GeODC(II)}]}{[\mathrm{Ge}]}$ ratio. By the same comparison we note also that: in D3 samples the final concentration of Ge(1) defects is less than in the sample of reference [15] having the same Ge doping level; for sample B3 the final Ge(1) concentration is about the same of the analogous sample of reference [15]; the sample A3 has a final Ge(1) concentration larger than in the corresponding sample of reference [15] doped with 10^4 ppm of Ge.

These findings, apparently contradictory, can be clarified by the following considerations on the presence of GeODC(II) centers in the samples. As noted above, the GeODC(II) defects supplies additional a-type electrons for the generation of Ge(1) centers. On this basis, one could expect a larger effectiveness in creating Ge(1) in more oxygen-deficient samples. Nevertheless for such samples, it is reasonable also to expect, on the basis of a larger lack of oxygen at a fixed Ge-doping, a minor number of fourfold coordinated Ge atoms capable to trap electrons for generating Ge(1) defects, for example due to an environment preventing the necessary relaxation so decreasing the effectiveness of the electron trapping process [24,25]. These considerations bring to expect a less effective generation of Ge(1) defect in oxygen deficient samples. Probably, it is the balance of these two opposite properties that determines the final Ge(1) concentrations in our samples.

In the above scheme, regarding the experimental data reported in reference [15], we conclude that in those samples, analogously to A1 and A2 samples, the final Ge(1) concentration was fixed by the exhaustion of donors of b-type electrons, since the contribution of a-type electrons was too low ($\frac{[\mathrm{GeODC(II)}]}{[\mathrm{Ge}]} \sim 10^{-4}$). By comparing the data reported in Figure 5b with the previous ones of reference [15], we conclude that in samples C3 and D3 the GeODC(II) concentrations ($\leqslant 7 \times 10^{16}$ centers cm^{-3}) are too low for supplying a relevant number of additional a-type electrons and the oxygen deficiency plays only the role of inhibiting the Ge(1) formation. In B3 sample, where the GeODC(II) concentration is $\sim 4.5 \times 10^{17}$ cm^{-3}, the opposite roles of enhancing and inhibiting the Ge(1) generation played by oxygen deficiency are almost balanced. Finally in A3 sample (GeODC(II) concentration $\sim 5 \times 10^{18}$ cm^{-3}) the GeODC(II) centers supplies a number of a-type electrons sufficient to overcome the inhibition effect and to increase the final Ge(1) concentration with respect to an analogous Ge-doped sample not oxygen deficient.

5 Conclusion

We have studied the γ irradiation effects on sol-gel Ge doped silica samples with Ge content up to 10^4 ppm mol and with different oxygen deficiency estimated by the GeODC(II)/Ge ratio. By detecting the paramagnetic induced defects using EPR measurements we have found that Ge(2) centers generation depends on the GeODC(II) centers confirming that the latter are the precursors of Ge(2). At the same time we have found the lack of correlation between Ge(1) and Ge(2) generation. As regard the E'-Ge defects, we have found a dependence from oxygen deficiency but we have also evidenced that it is not the only relevant feature in particular at doses above 10^4 Gy.

Our data suggest that the oxygen deficiency influences the Ge(1) centers generation and some peculiarities have been found suggesting that the radiation sensitivity (limit concentration value) in high oxygen deficient materials depends on the Ge content. Furthermore, for Ge(1) defects we have showed that high radiation sensitivity can be obtained at low Ge concentration in low oxygen deficient materials, a relevant feature for the use of Ge doped silica in photosensitive applications.

We thank G. Buscarino, M. Cannas, M. Leone, F. Messina for useful discussions. Technical assistance by G. Napoli and G. Tricomi is gratefully acknowledged.

References

1. *Defects in SiO_2 and related dielectrics: Science and Technology*, edited by G. Pacchioni, L. Skuja, D.L. Griscom, (Kluwer Academic Publishers, Dordrecht, 2000), p. 453

2. M. Leone, S. Agnello, R. Boscaino, M. Cannas, F.M. Gelardi, in *Silicon-based Materials and Devices*, edited by H.S. Nalwa (Academic Press, San Diego, 2001)
3. V.B. Neustruev, J. Phys. Condens. Matter **6**, 6901 (1994)
4. L. Skuja, J. Non Cryst. Sol. **149**, 77 (1992)
5. T.E. Tsai, E.J. Friebele, M. Rajaram, S. Mukhapadhyay, Appl. Phys. Lett. **64**, 1481 (1994)
6. V.B. Sulimov, V.O. Sokolov, E.M. Dianov, B. Poumellec, Quant. Electr. **26**, 988 (1996)
7. A. Zatsepin, V.S. Kortov, H.-J. Fitting, J. Non Cryst. Sol. **351**, 869 (2005)
8. F. Meinardi, A. Paleari, Phys. Rev. B **58**, 3511 (1998)
9. R.F. Cuevas, E.H. Sekiya, A. Garcia-Quiroz, E.C. Da Silva, C.K. Suzuki, Mat. Sci. Eng. B **111**, 135 (2004)
10. R.F. Cuevas, E.H. Sekiya, A. Garcia-Quiroz, E.C. Da Silva, C.K. Suzuki, Nucl. Instrum. Methods Phys. Res., Sect. B **247**, 285 (2006)
11. Y.Watanabe, H. Kawazoe, K. Shibuya, K. Muta, Jap J. Appl. Phys. **25**, 425 (1986)
12. E.V. Anoikin, A.N. Guryanov, D.D. Gusovskii, V.M. Mashinskii, S.I. Miroshnichenko, V.B. Neustruev, V.A. Tikhomirov, Y.B. Zverev, Sov. Ligtht. Comm. **1**, 123 (1991)
13. E.J. Friebele, D.L. Griscom, G.H. Sigel Jr, J. Appl. Phys. **45**, 3424 (1974)
14. M. Fujimaki, T. Watanabe, T. Katoh, T. Kasahara, N. Miyazaki, Y. Ohki, Phys. Rev. B **57** 3920 (1998)
15. S. Agnello, R. Boscaino, M. Cannas, F.M. Gelardi, F. La Mattina, S. Grandi, A. Magistris, J. Non Cryst. Sol. **322**, 134 (2003)
16. S. Agnello, R. Boscaino, M. Cannas, F.M. Gelardi, Phys. Rev. B **64**, 174423 (2001)
17. S. Grandi, P. Mustarelli, S. Agnello, M. Cannas, A. Cannizzo, J. Sol-Gel Science and Tech. **26**, 915 (2003)
18. H.Hosono, Y. Abe, D.L. Kinser, R.A. Weeks, K. Muta, H. Kawazoe, Phys. Rev. B **46**, 11445 (1992)
19. L. SKuja, J. Non Cryst. Sol. **239**, 16 (1998)
20. H. Nishikawa, in *Silicon-based Materials and Devices*, edited by H.S. Nalwa (Academic Press, San Diego, 2001)
21. M. Yamaguchi, K. Saito, A.J. Ikushima, Phys. Rev. B **66**, 132106 (2002)
22. M. Takahashi, H. Shigemura, Y. Kawamoto, J. Nishii, T. Yoko, J. Non Cryst. Sol. **259**, 149 (1999)
23. D.L. Griscom, Nucl. Instrum. Methods Phys. Res., Sect. B **1**, 481 (1984)
24. G. Pacchioni, C. Mazzeo, Phys. Rev. B **62**, 5452 (2000)
25. J. Du, L.R. Corrales, K. Tsemekhman, E.J. Bylaska, Nucl. Instrum. Methods Phys. Res., Sect. B **225**, 188 (2007)